

CONVECTIVE HEAT TRANSFER COEFFICIENT IN COMPARTMENT FIRES

J. G. Qunitiere* and P. S. Veloo**

jimq@umd.edu

*University of Maryland, College Park, MD USA

**University of Southern California, Los Angeles, CA USA

Abstract

Heat transfer to compartment surfaces was measured in fully developed fire experiments. The experiments involved scaled-compartments ranging from 1/8th to 3/8th of 2.54 m, full-scale height. Gas temperatures reached 1000 °C, and total surface heat flux could reach 200 kW/m², with convection accounting for about 25 %. A combination of thermopile cold sensor, plate sensor and gas and wall temperatures were used to separate convective and radiative heat flux in order to measure the convective heat transfer coefficient. The convective heat transfer coefficient has been correlated against temperature rise within the compartment for both the flaming and cooling after extinction phases.

Introduction

Convection heat transfer is usually downplayed in fire applications, as radiation dominates the burning rate for fires above 1 m in scale. In the early stage of convection is appreciated to be more important, especially in the activation of thermal alarms and sprinklers. Yet in fully developed fire, the role of convection has not been actively explored. Indeed, in the consideration of the effect of fire on structures (e.g. beams and columns), the convection heat transfer coefficient is usually taken as some extrapolation of normal heat transfer. This is especially troubling when the cooling period following extinction in a fire is an empirical factor as a constant temperature rate. Knowledge of the convective heat transfer coefficient could serve to offer a better model.

Very limited studies exist on the heat transfer coefficient in fire applications. Zukoski and Kubota [1] used a thin plate calorimeter to measure and correlate the convective heat transfer coefficient to a ceiling due to fire plume impingement. They correlated the results in terms of the dimensionless energy release rate, Q^* . Later Tanaka and Yamada [2] studied fires in nearly closed cubic compartments of 0.5 and 1.5 m to measure the overall heat transfer coefficient. They formed a correlation in terms of Q^* , but also noted a dependency on the temperature rise in the compartment. As temperature is the driving force for compartment flow, and convective heat transfer is velocity and scale dependent, we later explored that correlation approach. While the Tanaka & Yamada results are for low temperature, we will explore to the high temperature range of fully developed fires.

The compartment experiments of our study spring from a bigger study that explored the use of scale models in predicting the effect of fire on structures [3]. These fires involved wood cribs and compartment scales of 1/8, 1/4 and 3/8 of a benchmark compartment of 3.76 x 3.76 x 2.54 m high.

Measurements of heat flux were made with a commercial thermopile water cooled gage, and a fabricated thin plate gage. Further details can be found in Veloo [4]. The use of a plate thermometer has been used before in fire applications [1,5,6], but not this fully developed compartment fire scenario to obtain the heat transfer coefficient.

First, we will explain our plate sensor design. Then we will describe the methodology used to measure the heat transfer coefficient in the compartment fires, show some results, and then the final dimensionless correlation.

Plate Sensor Design

The concept of the plate sensor is to establish by calibration its backside substrate heat loss, its time response, and its effective heat capacity. Then its implementation is to treat it like a first-order linear time response device and correct its “steady” reading to the measurement. An examination of the calibration process will reveal the details of this process.

The sensor design is depicted in Figure 1, with the plate of 2 mm thick steel blackened by soot and paint giving an emissivity of about 0.9. The temperature of the plate is recorded over time as its front surface is exposed to a heat source and its backside is heavily insulated.

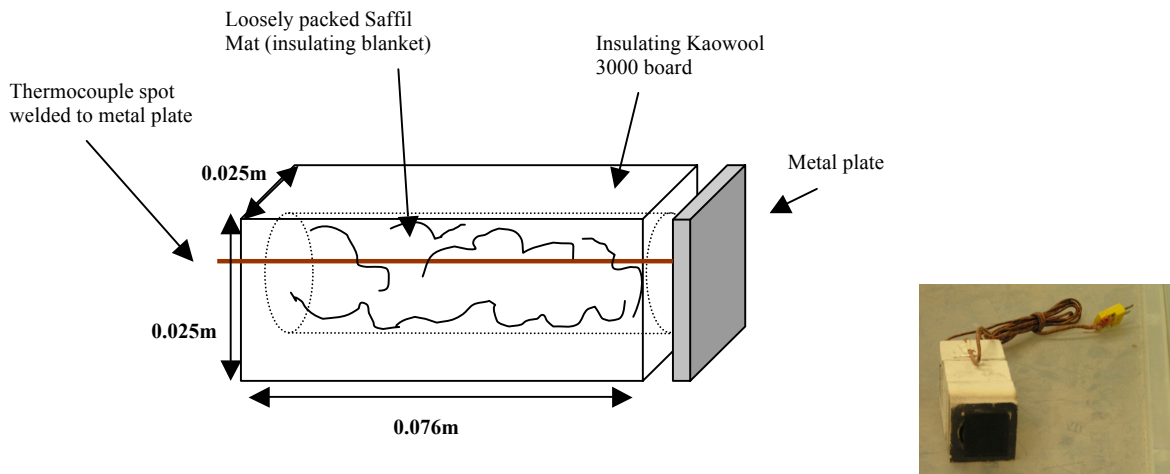


Figure 1. Metal Plate Sensor

The calibration arrangement is shown in Figure 2 in which incident radiant heat from a high temperature gas fired panel is imposed on an inert board containing the plate sensor and a known water-cooled thermopile heat flux gage. The plate sensor response is given by Eq. (1)

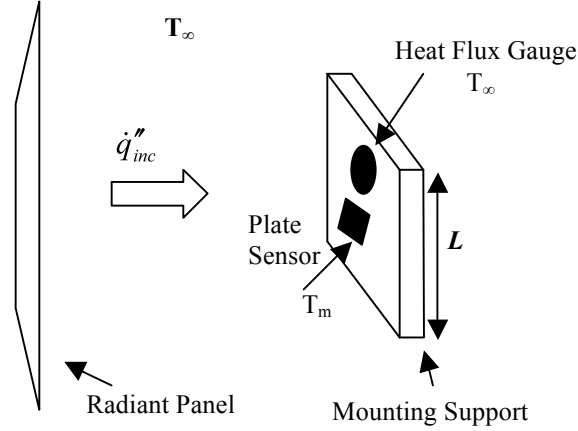


Figure 2. Calibration arrangement

Where incident radiant heat flux is felt from the panel and heat loss is by re-radiation, convection to the ambient, and heat conduction into insulation.

$$\left(\frac{mc}{A}\right)_m \frac{dT_m}{dt} = \alpha_m \dot{q}''_{inc} - \sigma \epsilon_m (T_m^4 - T_\infty^4) - h_{c,plate} (T_m - T_\infty) - \dot{q}''_{cond} \quad (1)$$

The subscript-m refers to the metal plate, and the full description of symbols is listed in the nomenclature. To not disrupt the flow of the text, all terms are not explicitly defined here, but hopefully their meaning is fairly obvious.

The conduction loss can be determined at steady state from measurements of incident heat flux, plate temperature, taking the absorptivity and emissivity as 0.9, and estimating the convective heat transfer coefficient from natural convection vertical plate correlations. As this heat loss into the insulation is expected to be relatively small, such steady estimates are reasonable even applied in the transient period. Further, the conductive loss is estimated as linear in plate to ambient temperature difference, i.e.

$$h_k = \frac{\alpha_m \dot{q}''_{inc} - \sigma \epsilon_m (T_m^4 - T_\infty^4) - h_{c,plate} (T_m - T_\infty)}{(T_m - T_\infty)} \quad (2)$$

Figure 3 shows that this can be taken as a function of the incident heat flux, and will be used in application later in the compartment measurements. In essence, above an incident heat flux of 5 kW/m², the h_k is 13.1 W/m²-K. So in this approximate fashion a conduction heat loss is estimated in the plate measurement.

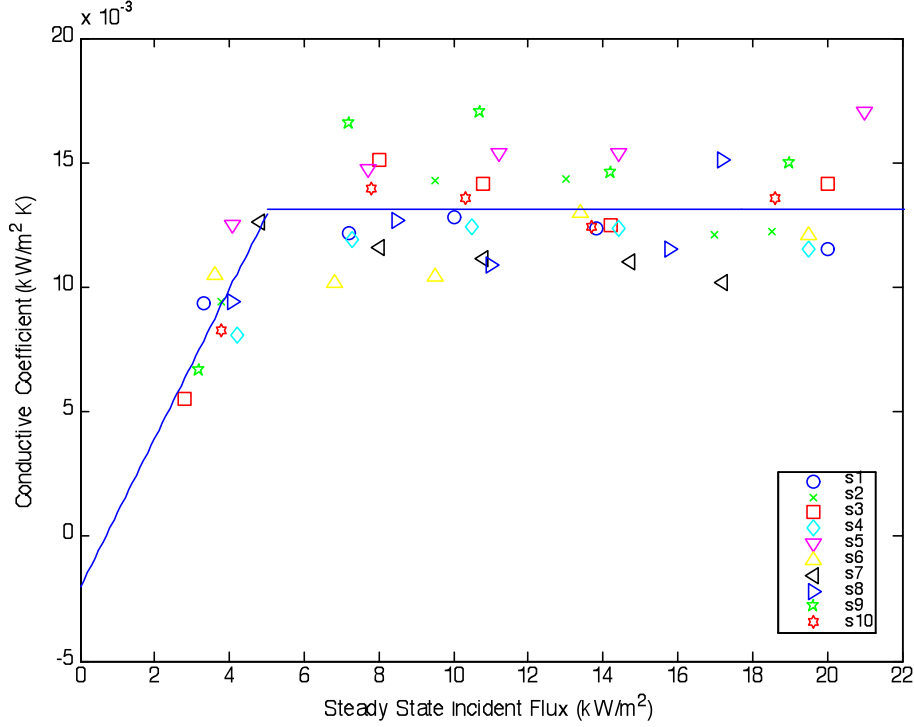


Figure 3. Conduction coefficient as a function of incident heat flux

In addition to linearizing the conduction loss with temperature, the re-radiation is treated in a similar way. In this way, Eq. (1) can be rewritten as

$$\left(\frac{mc}{A}\right)_m \frac{dT_m}{dt} = \alpha_m \dot{q}_{inc} - h_{eff}(T_m - T_\infty) \quad (3)$$

where h_{eff} represents:

$$h_{eff} = h_c + h_k + \sigma \epsilon_m (T_m^2 + T_\infty^2)(T_m + T_\infty). \quad (4)$$

Now consider the measured metal plate sensor heat flux is taken as

$$\dot{q}_m'' = \sigma \epsilon (T_m^4 - T_\infty^4) + h_c (T_m - T_\infty) + h_k (T_m - T_\infty) \equiv h_{eff} (T_m - T_\infty). \quad (5)$$

In this calibration mode, the plate reading can be derived from the instantaneous temperature measurement according to the substitution into Eq. (5). However, if we wish to derive the incident radiant heat flux from this plate reading, we must revert to the following equation that follows from the definition of \dot{q}_m'' in Eq. (5) and Eq. (3):

$$\frac{(mc)_m}{A_m h_{eff}} \frac{d\dot{q}_m''}{dt} + \dot{q}_m'' = \alpha_m \dot{q}_{inc}. \quad (6)$$

The terms embracing the coefficient of the derivative in Eq. (6) is the time constant of the device, t_r , and need not be computed from its components. More empirically, the time constant can be derived from the calibration tests. Applying an incident radiant heat flux, and recording the plate temperature over time allows the computation of \dot{q}_m'' and its time derivative, then t_r can be found from Eq. (6). Its value as a function of plate temperature is shown in Figure 4; it is clearly a function of temperature due to its dependence on h_{eff} .

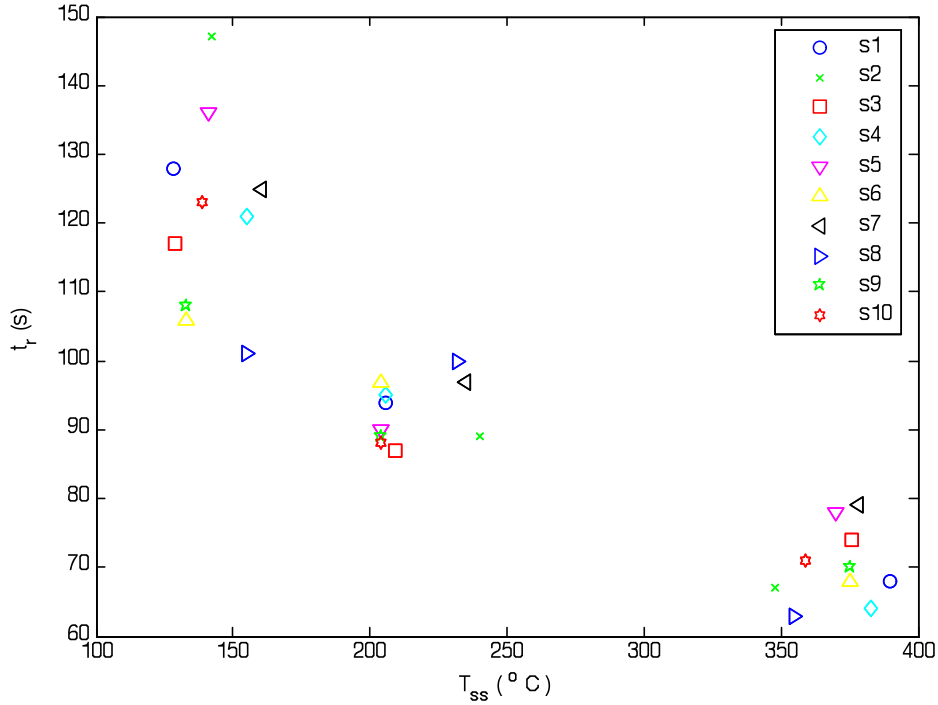


Figure 4. Response time for the heat flux equation, Eq. (6)

However, the remainder of the time constant term is primarily a constant, despite some temperature effect in the specific heat. This is shown by processing the data in Figure 4 with the corresponding h_{eff} term. Figure 5 shows the constancy of mc/A , and it will be taken as a constant for the plate gage as $3.21 \text{ kJ/m}^2\text{-K}$.

The heat capacity per unit area and the heat loss by conduction through the back insulation are taken as two properties constant of the plate gage: mc/A is $3.21 \text{ kJ/m}^2\text{-K}$ and h_k is $13.1 \text{ W/m}^2\text{-K}$ for most applications. The gage can now be applied to other applications, such as heating in a compartment in which the incident heat flux is from convection and radiation. The application of Eq. (6) is the operator of the gage and will give the incident heat flux (radiation plus convection in the compartment). This process will be explicitly laid out in the next section. However, to see that the process can be applied to the calibration application in which the incident radiant heat flux is constant for a run, Figure 7 shows the results of the of the direct measure of gage and the incident flux computed by Eq. (6).

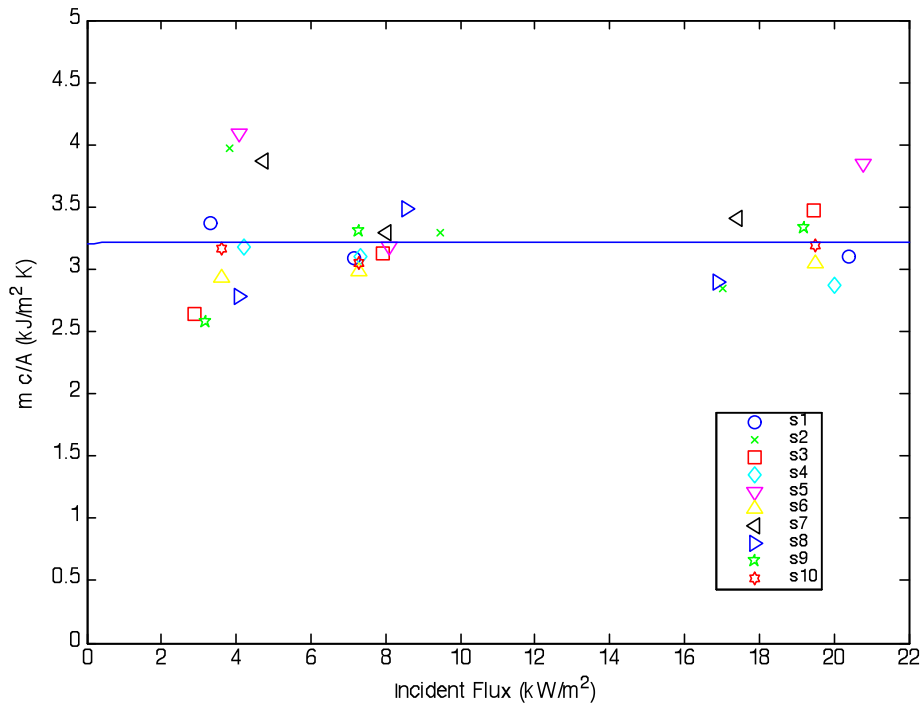


Figure 6. Heat capacity per unit area of plate gage

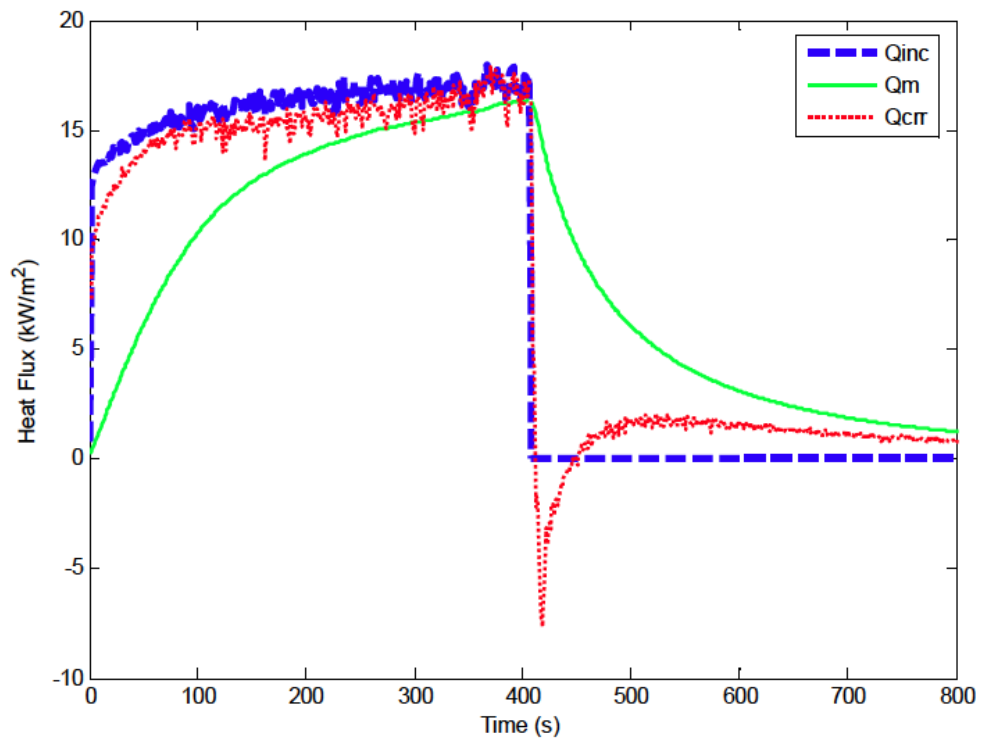


Figure 7. Example of plat gage giving incident radiant heat flux

Compartment Heat Flux Measurements and Methodology

Three scale compartment sizes were used in the measurements of heat flux. They consist of heat flux by the plate gage and by a water-cooled thermopile gage, along with local measurements of gas and compartment wall temperature. A depiction of this arrangement is shown in Figure 8.

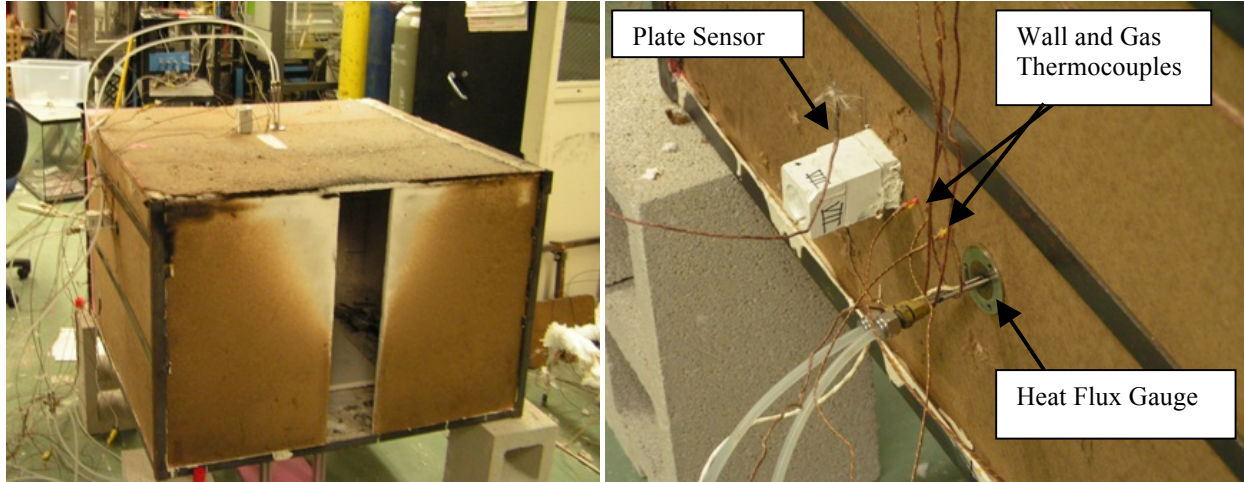


Figure 8. Arrangement of heat flux and temperature measurements

Three locations were used: ceiling and upper and lower wall. Herein, we will not discriminate among these measurements, as substantive differences were not indicated in these fully developed fires. Figure 9 is an indication of the gas temperature levels measured, and Figure 10 is illustrative of the heat flux levels. Levels attained 1100 °C and 200 kW/m².

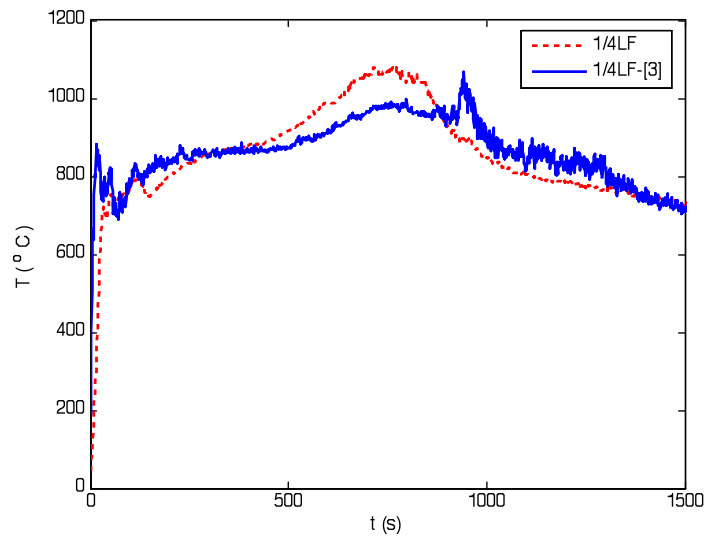


Figure 9. Illustration of compartment gas temperatures

The metal plate sensor measured flux in a compartment fire is given by Eq. (7).

$$\left(\frac{mc}{A}\right)_m \frac{dT_m}{dt} + \dot{q}''_{cond} + \varepsilon_m \sigma T_m^4 = \dot{q}''_{fire,r} + h_{fire,c} (T_g - T_m). \quad (7)$$

Analogous to Eq (4), here h_{eff} is taken as

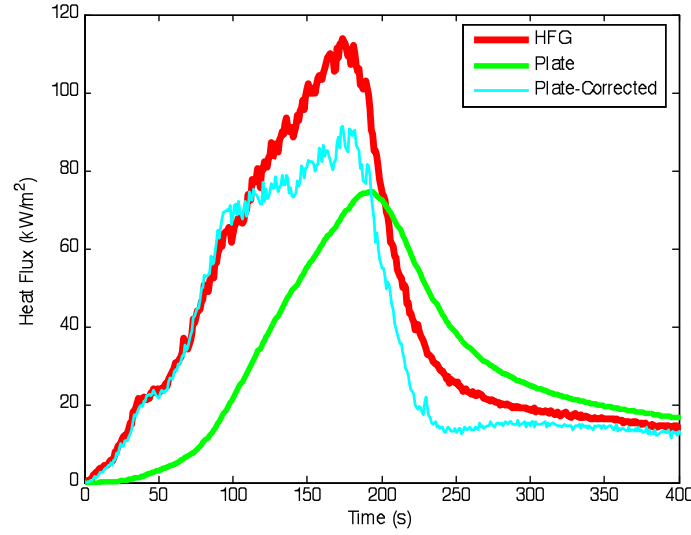


Figure 10. Illustration of compartment heat flux levels

$$h_{eff,c} = h_k + \sigma \epsilon_m (T_m^2 + T_\infty^2)(T_m + T_\infty), \quad (8)$$

as there is no convective loss term, but now a convective addition handled in the incident flux. Taking the plate heat flux (uncorrected) as

$$\dot{q}_m'' \equiv h_{eff,c} (T_m - T_\infty); \quad (9)$$

Then it follows from Eqns. (7) and (8) that

$$t_{r,fire} \frac{d\dot{q}_m''}{dt} + \dot{q}_m'' = \dot{q}_{m,in}'', \text{ with } t_{r,fire} \equiv \left(\frac{mc}{A} \right) / h_{eff,c}. \quad (10)$$

The incident heat flux to the plate sensor, $\dot{q}_{m,in}''$, is equal to the total incident radiation and convection heat flux from the compartment fire to the metal plate sensor (right side of Eq. (7)):

$$\dot{q}_{m,in}'' = h_{fire,c} (T_g - T_m) + \dot{q}_{fire,r}'', \quad (11)$$

and correspondingly the incident heat flux to the water-cooled heat flux gage (HFG) is

$$\dot{q}_{HFG}'' = h_{fire,c} (T_g - T_\infty) + \dot{q}_{fire,r}''. \quad (12)$$

The difference between the heat flux gauge measured flux, Eq. (12), and the metal plate sensor measured flux, Eq. (11), gives the convective heat transfer coefficient as

$$h_{fire,c} = \frac{\dot{q}_{HFG}'' - \dot{q}_{m,in}''}{(T_m - T_\infty)} \quad (13)$$

Figure 10 shows these differences between the HFG and the corrected plate or incident plate heat flux.

Convective Heat Transfer Coefficient

An illustration of the computed heat convective heat transfer coefficient, per Eq. (13), along with processing the parameters of Eqns. (7) – (13), is shown in Figure 11. From its order of magnitude (say $50 \text{ W/m}^2\text{-K}$) and a maximum incident heat flux of 200 kW/m^2 at gas temperatures of $1000 \text{ }^\circ\text{C}$, suggests a convective portion of the total as about 50 kW/m^2 . Hence in these fires convection can be p to 25 % of the total heat flux received by a flat surface in the compartment.

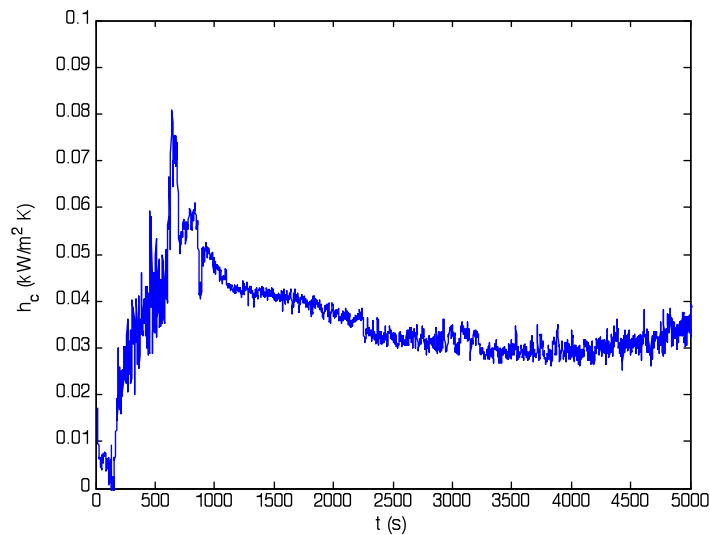


Figure 11. Illustration of determined convective heat transfer coefficient during a fire

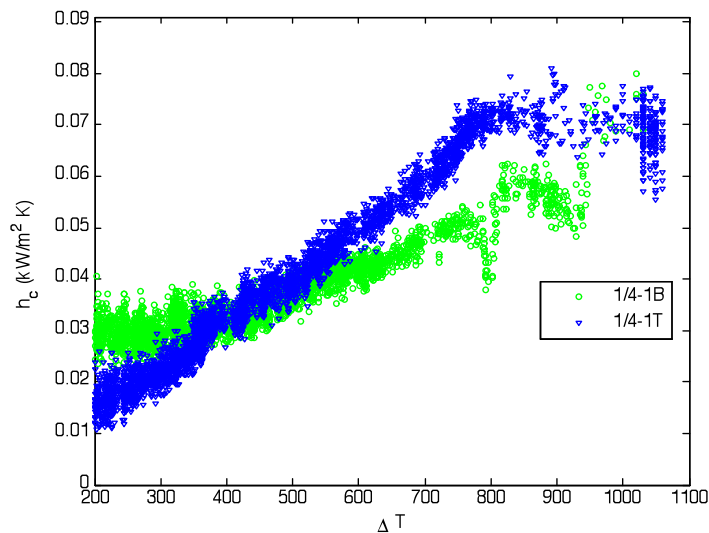


Figure 12. Illustration of the heat transfer coefficient at two measuring stations, after extinction

These convective heat transfer coefficient results were arranged according to their corresponding local gas temperatures recorded over time in a given run. Figure 12 gives some results for two of the measuring points in a compartment fire. While some differences exist for the locations, for these fully developed large fires, a definitive trend with location was not perceived. Then all of these results were presented, for both the wall and ceiling locations, in total in terms of the temperature rise over ambient. This temperature difference is the driving force for flow into the compartment opening.

The heat transfer coefficient is seen to increase with temperature difference. As scale was varied in these experiments, the effect of scale was accounted for by considering a dimensionless heat transfer coefficient as the Stanton number expressed in terms of a characteristic velocity in natural convection. The characteristic length, l , scale was taken the height of the compartment. Figures 13 and 14 show the totality of results plotted for both the burning period and the cooling or extinction period following. It is seen that the data of Tanaka and Yamada [2] for small fires complies with the correlation. Fits of these data indicate approximate formulas for the before extinction case as:

$$\frac{h_c}{\rho_\infty c_p (gl)^{1/2}} = \begin{cases} 2.03 \times 10^{-3} & \frac{\Delta T}{T_\infty} < 2 \\ 16.00 \times 10^{-3} \frac{\Delta T}{T_\infty} & \frac{\Delta T}{T_\infty} \geq 2 \end{cases} \quad (14)$$

and for after extinction as:

$$\frac{h_c}{\rho_\infty c_p (gl)^{1/2}} = 9.87 \times 10^{-3} \frac{\Delta T}{T_\infty}. \quad (15)$$

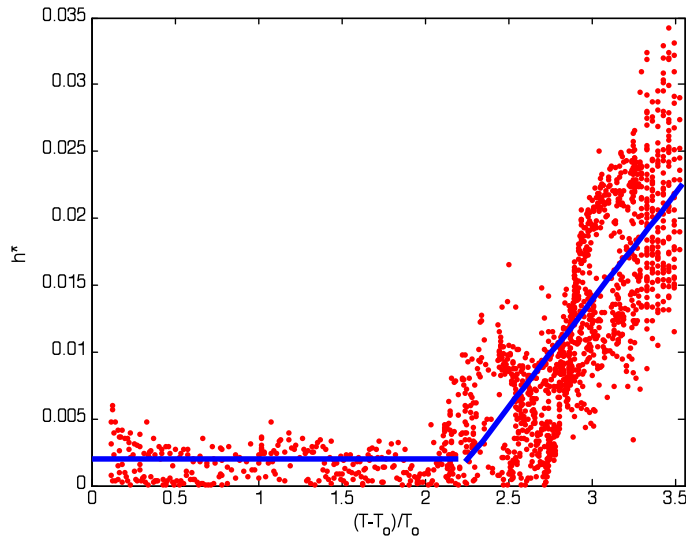


Figure 13. Dimensionless heat transfer coefficient during flaming

Summary and Conclusions

Using a heated plate heat flux gage and a water-cooled gage, the convective heat transfer coefficient was measured and correlated over a range of temperatures in flaming and cooling periods for compartment fires. Heat flux could attain levels of 100 to 200 kW/m² with convection accounting for up to 25 %. The results could be applied to improve empirical estimates of the rate of cooling in compartment fires, and its impact on structure integrity.

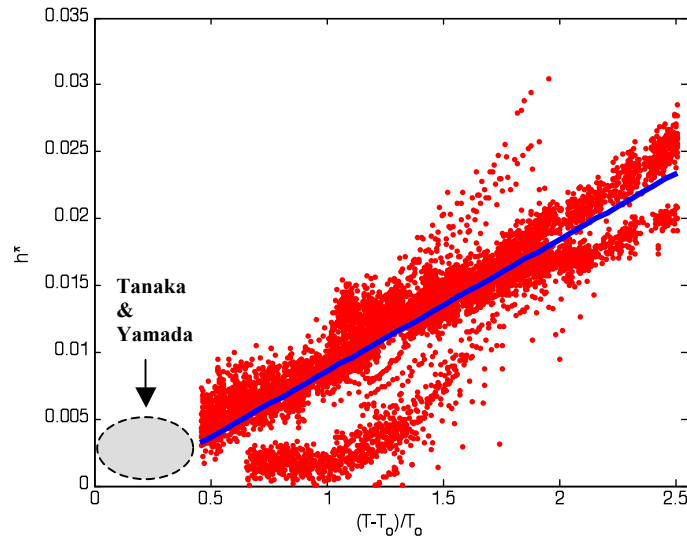


Figure 14. Dimensionless heat transfer coefficient for the cooling or extinction phase

Nomenclature

A	Area
c	Specific Heat
g	Gravity
h_c	Convective Heat Transfer Coefficient
\dot{q}''	Heat Flux per Unit Area
t	Time
T	Temperature
α_m	Absorptivity Metal Plate Sensor
ε	Emissivity
ρ	Density

Subscripts

c	pertains to convection
HFG	pertains to water-cooled sensor
in	pertains to incident heat flux
m	pertains to plate sensor
r	pertains to radiation

References

- [1] Zukoski, E. E., Kubota, T., “An Experimental Investigation of the Heat Transfer from a Buoyant Gas Plume to a Horizontal Ceiling – Part 2 Effects of Ceiling Layer”, National Bureau of Standards (U.S.), NBS-GCR-77-98, 1975
- [2] Tanaka, T., Yamada, S., “Reduced Scale Experiments for Convective Heat Transfer in the Early Stages of Fire”, *Int. J. Eng. Performance-Based Fire Codes*, 1999, **1**(3), 196-203.
- [3] Perricone, J., Wang, M., Quintiere, J. G., “Scale Modeling of the Transient Thermal Response of Insulated Structural Frames Exposed to Fire”, *Fire Technol.*, v. 44, n. 2, June 2008.
- [4] Veloo, P. S., “Scale Modeling of the Transient Behavior of Heat Flux in Enclosure Fires”, MS Thesis Dept. Fire Prot. Engrg. Univ. of Maryland, April 2006.
- [5] Wickstrom, U., “The plate thermometer - a simple instrument for reaching harmonized fire resistance tests”, *Fire Technol.*, v. 30, n. 2, pp195-208.
- [6] Tofilo, P., Delichatsios, M. A., Silcock, G. W. H., *Effective of Fuel Sootiness on the Heat Fluxes to the Walls in Enclosure Fires*, 8th International Symposium on Fire Safety Science, 2005.